Gene Expression

DOI: 10.1002/anie.201201495

Drawing Sticky Adeno-Associated Viruses on Surfaces for Spatially Patterned Gene Expression**

Eunmi Kim, In Taek Song, Slgirim Lee, Jung-Suk Kim, Haeshin Lee, and Jae-Hyung Jang**

In developing tissues, the spatially controlled secretion of extracellular signals creates biointerfaces that modulate cellular processes of differentiation, proliferation, and migration, and provide molecular cues to organize the structure of tissues.[1–4] Systems that control spatial distribution of extracellular molecules on substrates have been developed in order to induce patterned expression of intracellular inductive factors.[1,5,6] Alternatively, spatially patterned gene delivery has been employed to overcome limitations found in protein delivery: short protein half-life and systemic toxicity.[7–9] The development of in vitro model systems that mimic the spatial control of gene expression in tissues or organs is critical to elucidate a variety of biological mechanisms. However, the majority of gene delivery systems rely on simple additions of gene carriers directly to media, which are inherently limited in their ability to spatially control gene expression.

Advances in micro- and nanofabrication technologies have enabled researchers to control locations of gene vectors on surfaces.[10,11] Existing methods include microfluidics,[8,12] surface coating,[13] and self-assembly.[14] In general, the techniques involve multiple laborious procedures, typically chemical activation of substrates, resist depositions, pattern generation using a photomask, and gene vector immobilization. Furthermore, expensive equipment is often necessary.

Unlike the aforementioned complex processes, this study describes a simple, versatile approach for spatially patterned gene delivery inspired by adhesion of marine mussels. Catecholamine, the key adhesive moiety found in the specialized adhesive proteins of *mytilus edulis*, was used to formulate "sticky" viruses. The adhesive catecholamine polymer used in this study is poly(ethylenimine)-catechol (PEI-C), which has been used for material-independent layer-by-layer assembly and mechanical reinforcement of carbon nanotube fibers.[15,16] The adeno-associated virus (AAV), which is a safe and efficient parvovirus,[17] was complexed with the PEI-C. Because of the underwater adhesive property of PEI-C, the AAV vector complexed with the PEI-C became a highly sticky virus that can stably adhere onto surfaces. Most importantly, by using the sticky viral vectors, we were able to use a micropipette as a "pen" to create viral patterns on substrates. This "gene-vector drawing" technique bypasses laborious multiple steps and can thus be a versatile platform to control gene expression for the establishment of complex tissues.

Branched PEI was conjugated with 3-(3,4-dihydroxyphenyl) propionic acid (DPA) to generate PEI-C, which provides sticky viral vectors (Figure 1 A). A novel virus, AAV r3.45, which was specifically designed for neuronal cell

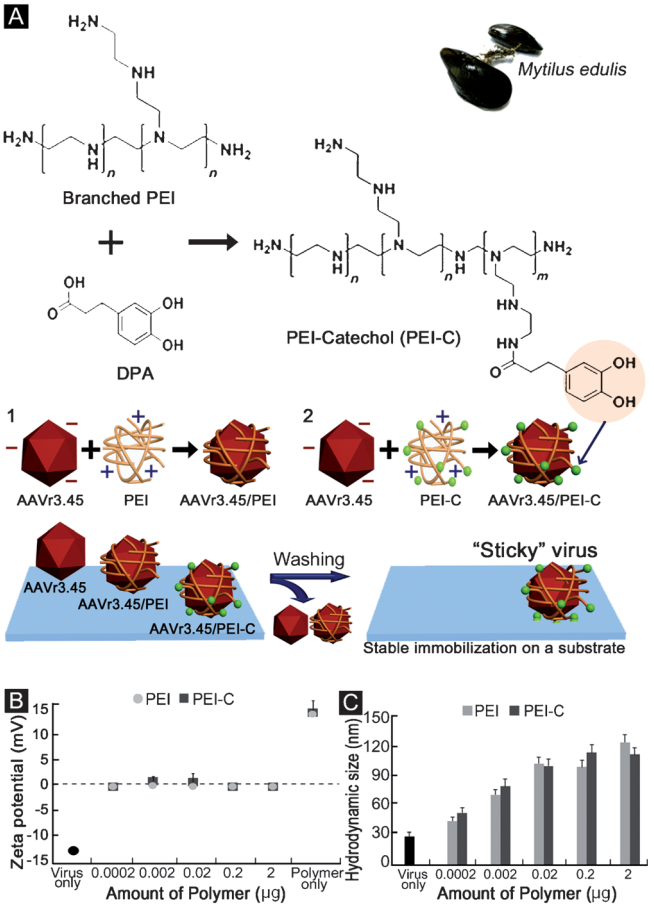

Figure 1. Formulation and characterization of the AAV/PEI-C hybrid vectors. A) Schematic illustration of the structure of PEI-C, hybrid vectors, and stable immobilization of sticky virus. B) Net charges of hybrid vectors. C) Hydrodynamic sizes of the hybrid vectors.

[*] E. Kim, S. Lee, J. S. Kim, Prof. J. H. Jang
Department of Chemical and Biomolecular Engineering
Yonsei University, Seoul, 120-749 (Korea)
E-mail: j-jang@yonsei.ac.kr
I. T. Song, Prof. H. Lee
Department of Chemistry, KAIST, Daejeon, 305-701 (Korea)
E-mail: haeshin@kaist.ac.kr

[**] This work was supported by National Research Foundation (NRF) grant funded by the Korea government (MEST) through the Active Polymer Center for Pattern Integration (No. R11-2007-050-00000-0 to J.H.J.), the Human Resources Development of the Korea Institute of Energy Technology Evaluation and Planning (KETEP) grant funded by the Korea government Ministry of Knowledge Economy (No. 20104010100500 to J.H.J.), Pioneer Research Program, (2011-0001696 to H.L.), and Korea Biotech R&D Program (2011K000809 to H.L.).

Supporting information for this article is available on the WWW under http://dx.doi.org/10.1002/anie.201201495.

tropism in a previous study,[18] was employed as a gene carrier. The degree of catechol conjugation is the ratio of the amines that reacted with DPA to the total number of primary amines of PEI. UV/Vis absorption spectroscopy confirmed that the degrees of catechol conjugation were approximately 5.8 and 16%. This catechol conjugation does not result in significant reductions in the cationic properties of PEI and therefore maintains the capability of PEI to form complexes through electrostatic interactions with the negatively charged AAV (−12.5 mV; Figure 1B). Net charges of PEI and PEI-C (5.8 and 16% conjugation) were (12.85 ± 2.10), (13.21 ± 4.57), and (15.45 ± 6.99) mV, respectively ($P > 0.05$).

The AAV vectors were subsequently hybridized with PEI-C. The term hybrid originated from approaches that integrated viral vectors with the components widely utilized in nonviral vector delivery, such as PEI. The negative surface charge of AAVr3.45 is a driving force for the ability to form complexes with cationic PEI-C. As the mass of PEI-C was increased, the net charges of the AAV/PEI-C complexes were neutralized (Figure 1B). The hybrid vectors maintained neutral charges presumably because of either the exclusion of agglomeration complexes that contained larger quantities of cationic polymers upon filtration, or no additional attachment of PEI-C for the functionalized virus surface.

The increased size of the hybrid vectors might be a result of the interactions between the PEIs and viruses. The differences in size between the viruses coated with either PEI or PEI-C were not significant (Figure 1C). In contrast, the effects of catechol moieties in PEI on physicochemical properties of the hybrid vectors were observed. As the degree of catechol conjugation of PEI was increased from 5.8 to 16%, enhanced vector aggregation was found, implying that the surface-exposed catechols contribute to interparticle interactions through catechol–catechol or catechol–amine adducts. As a result of these observations, the lower degree of catechol conjugation within PEI (i.e., 5.8%) was utilized for further study.

The direct addition of the AAV/PEI-C vectors to cells resulted in significantly enhanced cellular transduction compared with the unmodified vectors (Figure 2A,B). The complexation of viral vectors with a small quantity (0.2–2 ng) of PEI-C led to an approximately two-fold enhanced cellular transduction in HEK293T cells. In contrast, increases in the particle size appeared to influence cellular uptake, as decreases in cellular transduction were observed (Figure 2B). The ability of the AAV/PEI-C hybrid vectors to enhance cellular transduction is likely related to the enhanced interactions between receptor proteins. The majority of the unmodified virus and the AAV/PEI complexes eluted through a heparin column with NaCl concentrations between 350 and 550 mM (see Figure S1 in the Supporting Information). However, large fractions of the PEI-C hybrid vectors eluted with higher concentrations of NaCl (700–1000 mM; Figure S2), thus implying strong binding of the catechols to heparin.[19] The altered heparin affinities of the hybrid vectors may result in enhancement of cellular transduction compared with nonmodified AAVr3.45, possibly because of the reinforced interactions of the hybrid vectors with heparan sulfate proteoglycan (HSPG), which is prevalent on cellular membranes.

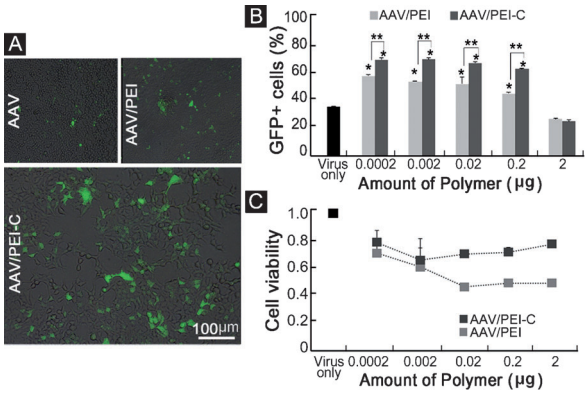

Figure 2. Cellular transduction of hybrid vectors. A) Representative images of HEK293T infections. B) Percentage of GFP-expressing HEK293T cells two days after infection (genomic multiplicity of infection: 10^4). The symbols * and ** indicate significant differences compared with infections with AAVr3.45 and AAVr3.45/PEI, respectively ($P < 0.05$). C) Cell viabilities two days after infection (normalized to no infection).

High cationic charge densities of PEI chains are known to cause cellular toxicity. Therefore, the replacement of primary amines with catechols (5.8%) is likely to improve cell viability.[20] Consistent with these observations, the transduction of cells with the AAV/PEI-C hybrid reduced cellular toxicity (Figure 2C). In addition, an increase in the quantity of PEI-C did not cause toxicity to the cells, whereas an increase in the amount of PEI itself reduced cell viabilities.

The external exposure of catechols on the hybrid vectors enables robust immobilization of the vectors on the substrates. A number of AAV/PEI-C hybrid vectors remained on the tissue culture polystyrene plates after vigorous washing (Figure 3). Quantitative analysis demonstrated that approximately five-fold increases in fluorescence intensity were observed for the sticky viruses compared with the AAVr3.45, and 2.5-fold increases compared to the AAV/PEIs (Figure S3). The fluorescence intensity of the surface-bound hybrid vectors increased with the quantity of genomic particles (2.0×10^6 to 2.0×10^9 vg) and the amount of PEI-C (Figure 3B, C). This enhanced immobilization of vectors permitted an increase in the number of infected cells (Figure 3B, C), which unambiguously demonstrates the importance of adhesive properties of viral vectors for a controlled approach to gene delivery.

Simple drawing of the AAV/PEI-C viruses was achieved because of their adhesive properties (Figure 4A, B). The hybrid AAV vectors act as an 'ink' solution that remains stably on surfaces, and thus provides an opportunity for the spatial patterning of viruses. The advantage of this drawing technique is its simplicity in operation compared to widely implemented multi-step techniques, such as lithography techniques. The techniques often require expensive equipment, such as an inkjet or piezoelectric printer.[21] The loading of the AAV/PEI-C hybrid vector within a pipette tip followed by simply moving the tip to draw user-defined shapes (Y and U) resulted in the formation of continuous patterns of viral vectors, whereas delicate virus patterns with the AAVr3.45 alone and AAVr3.45/PEI could not be achieved (Figure 4B).

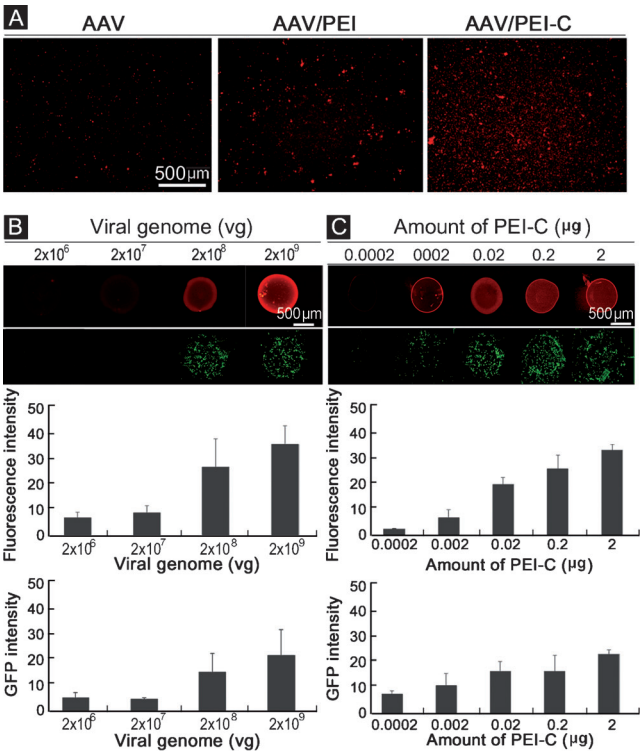

Figure 3. Immobilization of hybrid vectors on substrates. A) Fluorescence images of substrate-bound AAV hybrid vectors (Alexa Fluor 594 labeled). B) Fluorescence intensity of surface-bound hybrid vectors and infected cells with different quantities of viral genomic particles. HEK293T cells were infected by 2×10^6 to 2×10^9 viral genome (vg) particles formed with PEI-C (0.02 μg). C) Fluorescence intensity of surface-bound hybrid vectors and infected cells with different quantities of PEI-C. Cells were infected by 2×10^8 vg particles formed with various amounts of PEI-C.

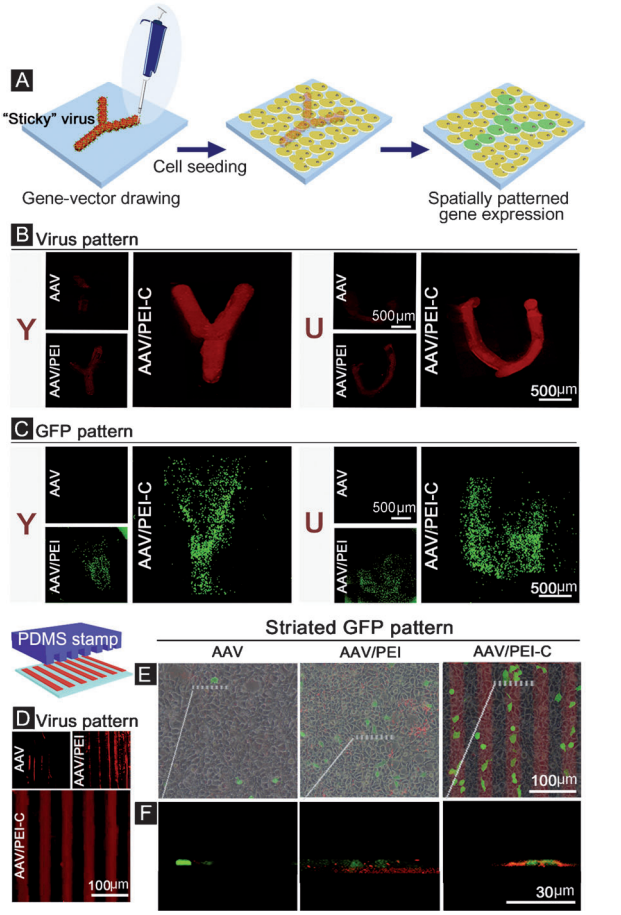

Figure 4. Spatially patterned gene delivery and expression. A) Use of the "sticky" hybrid vector system to obtain viral pattern and patterned gene expression. B) Viral patterns and C) patterned GFP expression demonstrated by simply moving the pipette tip containing the hybrid vectors (Y and U shape). D) Viral patterns and E) GFP expression demonstrated by the PDMS stamping technique. F) Confocal images taken in the *z* direction to present tightly bound hybrid vectors (red) around GFP-expressing cells (green) attached to a striated viral pattern.

Importantly, after the cells were seeded onto the spatially patterned hybrid vectors, subsequent gene expression corresponded to the drawn patterns (Figure 4C). These results therefore demonstrate the potential of the PEI-C hybrid vectors to guide directed or patterned gene expressions for tissue growth.[8]

The resolution of viral and gene expression patterns were easily improved by a poly(dimethylsiloxane) (PDMS) microstamp (30 μm). As shown in Figure 4D, well-defined patterns of hybrid vectors were obtained when the PDMS stamp was dipped into viral samples, and the ink solution was transferred to tissue culture plates. As expected, the majority of GFP-expressing cells were distributed along the viral patterns, thus implying that the detachment of the hybrid vectors for cellular uptake occurred upon contact with overlying cells (Figure 4E, right). The adsorption of the viral samples only or vectors complexed with PEI only did not generate viral patterns because of the lack of adhesive properties.

Confocal microscopy images taken in the *z* direction showed that the surface-bound AAV/PEI-C hybrid vectors within the striated patterned lines (30 μm) remained robustly attached to the surface (Figure 4F, right). However, the AAV/PEI vectors sparsely attached onto the surface of the tissue culture plates. (Figure 4F, middle). The decrease in viral adhesion resulted in poor viral patterns and gene expression (Figure 4E, middle). The *z* direction image of the virus-only control is not shown because the fluorescence signal of the virus was low (Figure 4F, left).

The demonstrated drawing technique is useful in creating a concentration gradient of a soluble neurotropic factor, such as nerve growth factor (NGF), that directs the guidance of neurite outgrowth of PC12 cells along the patterns (Figure 5A). Patterning the AAV hybrid vectors encoding NGF through the stamping technique resulted in the elongation of neurites of PC12 cells along the drawn viral patterns (Figure 5B, top), whereas the directions of neurite outgrowth by NGF-encoding AAV/PEI complexes were random (Figure 5B, bottom). The mean angle of neurites extended by AAV r3.45/PEI complexes demonstrated significantly larger deviation from the striped patterns than that of neurites extended by the sticky vectors ($P < 0.001$, Figure S4).

The ability of the AAV/PEI-C hybrid vectors to create viral patterns and concentration gradients of tissue inductive factors within a designated region was expanded to a conventional material, polycaprolactone (PCL), which is used extensively in tissue engineering applications. Hybrid vectors

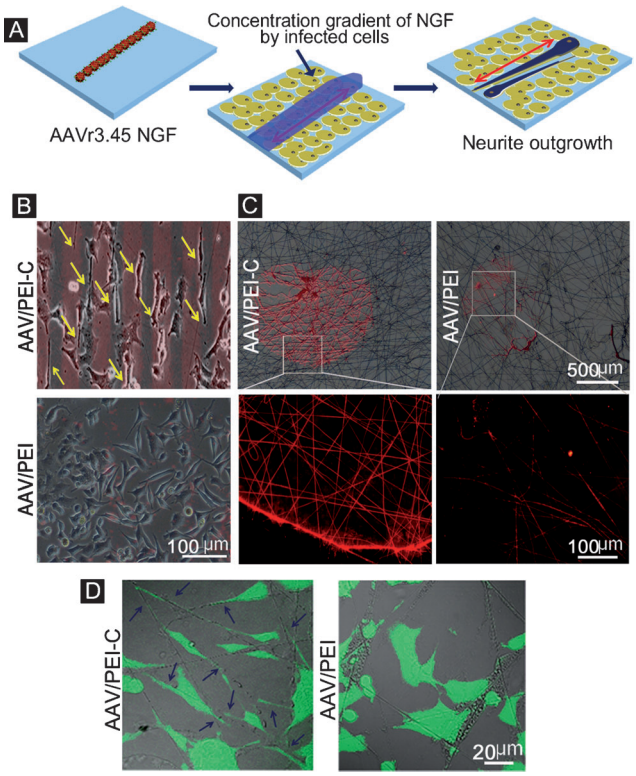

Figure 5. Spatially patterned neurite extensions. A) Schematic illustration of methodologies to induce neurite extensions. B) Neurite extensions along the viral patterns (AAV encoding NGF: red). C) Fluorescence images of hybrid vectors (red) immobilized on PCL electrospun nanofibers. D) Neurite extension from fluorescein diacetate labeled PC12 cells (green) along the PCL fibers (optical) containing surface-bound hybrid vectors encoding NGF.

encoding NGF were adsorbed onto nanofiber scaffolds fabricated by PCL electrospinning.[22] The PC12 cells were plated on the composites to mediate neuronal differentiation along the fibers. Consequently, the AAV/PEI-C hybrid vectors were spatially patterned along the PCL nanofibers (Figure 5C, left), and many portions of PC12 cells, which were successfully attached to the fibers, extended neurites along the fibers (Figure 5D, left). However, homogeneous adsorption of AAVr3.45/PEI vectors on the nanofibers was not achieved (Figure 5C, right), thus no substantial neurite outgrowth along the fibers was observed (Figure 5D, right). After advanced tools, such as the fabrication of aligned or three-dimensional nanofibrous scaffolds, have been employed for use with the gene-vector drawing technology, highly efficient systems that are capable of guiding three-dimensional tissue growth can be generated. The surface-presented catechols might effect on the neurite outgrowth. To disprove the hypothesis, green fluorescent proteins (GFP) encoding AAV/PEI-C vectors were used, and we observed that the catechols showed no effect on the neurite outgrowth.

In conclusion, a highly simple, versatile gene delivery strategy that exhibits the ability to spatially control gene expressions of mammalian cells has been successfully developed. Catecholamine polymers, PEI-C, inspired by the specialized adhesive moiety found in *mytilus edulis*, were utilized to functionalize surfaces of AAV viruses in order to create sticky viruses. Importantly, the presentation of the catechol moieties allows us to generate spatially controlled viral patterns on substrates by the simple "gene-vector drawing" technique. This technique directed neurite extension along predetermined patterns. Thus, this study indicates that the sticky hybrid vector system can be a general and versatile platform for the establishment of spatial gene patterning, with substantially reduced efforts and costs, for the facilitation of functional tissue organization.

Received: February 23, 2012
Published online: April 26, 2012

Keywords: adeno-associated virus · catechol · gene expression · spatially patterned gene delivery · viruses

[1] K. Stankunas, G. K. Ma, F. J. Kuhnert, C. J. Kuo, C. P. Chang, *Dev. Biol.* **2010**, *347*, 325–336.
[2] T. Dvir, B. P. Timko, D. S. Kohane, R. Langer, *Nat. Nanotechnol.* **2011**, *6*, 13–22.
[3] J. H. Jang, D. V. Schaffer, L. D. Shea, *Mol. Ther.* **2011**, *19*, 1407–1415.
[4] T. Serafini, S. A. Colamarino, E. D. Leonardo, H. Wang, R. Beddington, W. C. Skarnes, M. Tessier-Lavigne, *Cell* **1996**, *87*, 1001–1014.
[5] H. Hatakeyama, A. Kikuchi, M. Yamato, T. Okano, *Biomaterials* **2007**, *28*, 3632–3643.
[6] J. Lembong, N. Yakoby, S. Y. Shvartsman, *Tissue Eng. Part A* **2008**, *14*, 1469–1477.
[7] T. G. Park, J. H. Jeong, S. W. Kim, *Adv. Drug Delivery Rev.* **2006**, *58*, 467–486.
[8] T. Houchin-Ray, A. Huang, E. R. West, M. Zelivyanskaya, L. D. Shea, *J. Neurosci. Res.* **2009**, *87*, 844–856.
[9] T. Houchin-Ray, K. J. Whittlesey, L. D. Shea, *Mol. Ther.* **2007**, *15*, 705–712.
[10] R. B. Shmueli, D. G. Anderson, J. J. Green, *Expert Opin. Drug Delivery* **2010**, *7*, 535–550.
[11] H. Tavana, A. Jovic, B. Mosadegh, Q. Y. Lee, X. Liu, K. E. Luker, G. D. Luker, S. J. Weiss, S. Takayama, *Nat. Mater.* **2009**, *8*, 736–741.
[12] Y. Zhang, Z. Gazit, G. Pelled, D. Gazit, G. Vunjak-Novakovic, *Integr. Biol.* **2011**, *3*, 39–47.
[13] D. M. Pirone, L. Qi, H. Colecraft, C. S. Chen, *Biomed. Microdevices* **2008**, *10*, 561–566.
[14] A. K. Pannier, B. C. Anderson, L. D. Shea, *Acta Biomater.* **2005**, *1*, 511–522.
[15] S. Ryu, Y. Lee, J. W. Hwang, S. Hong, C. Kim, T. G. Park, H. Lee, S. H. Hong, *Adv. Mater.* **2011**, *23*, 1971–1975.
[16] H. Lee, Y. Lee, A. R. Statz, J. Rho, T. G. Park, P. B. Messersmith, *Adv. Mater.* **2008**, *20*, 1619–1623.
[17] Z. Wu, A. Asokan, R. J. Samulski, *Mol. Ther.* **2006**, *14*, 316–327.
[18] J. H. Jang, J. T. Koerber, J. S. Kim, P. Asuri, T. Vazin, M. Bartel, A. Keung, I. Kwon, K. I. Park, D. V. Schaffer, *Mol. Ther.* **2011**, *19*, 667–675.
[19] L. P. Zhu, J. Z. Yu, Y. Y. Xu, Z. Y. Xi, B. K. Zhu, *Colloids Surf. B* **2009**, *69*, 152–155.
[20] J. H. Jeong, S. H. Song, D. W. Lim, H. Lee, T. G. Park, *J. Controlled Release* **2001**, *73*, 391–399.
[21] C. G. Wilson, *Introduction to microlithography* (Eds.: L. F. Thompson, C. G. Willson, M. J. Bowden), 2nd ed., ACS, Washington, DC, **1994**.
[22] S. Lee, J. S. Kim, H. S. Chu, G. W. Kim, J. I. Won, J. H. Jang, *Acta Biomater.* **2011**, *7*, 3868–3876.

